DEPARTMENT OF GEOLOGY AND MINES

MINISTRY OF ECONOMIC AFFAIRS

Monitoring of Landslide at Arong, Moshi and Phongmey using GPS

Department of Geology and Mines

Monitoring Period: August 2015 to May 2017

DEPARTMENT OF GEOLOGY AND MINES

MINISTRY OF ECONOMIC AFFAIRS

Monitoring of Landslide at Arong, Moshi and Phongmey using GPS

Department of Geology and Mines

Monitoring Period: August 2015 to May 2017

ABOUT DEPARTMENT OF GEOLOGY & MINES (DGM)

Established in 1981 as Division initially and upgraded later to department, Department of Geology and Mines under Ministry of Economic Affairs is the only geo-scientific institution in the Kingdom of Bhutan mandated to carry out and manage geo-scientific and mining activities. Currently, the mandates of the department are fulfilled through four divisions namely: (1) Geological Survey Division; (2) Earthquake and Geophysics Division; (3) Mineral Development Division; and (4) Mining Division.

Contact Address: Department of Geology and Mines
Ministry of Economic Affairs
Royal Government of Bhutan
Thimphu: BHUTAN
P.O. Box: 173
Telephone: +975-2-323096
Web: www.moea.gov.bt

ABOUT THIS REPORT

This report is in accordance with the work plan of the Department of Geology and Mines, MoEA under the National Adaptation Programme of Action II (NAPA II) Project titled *'Addressing the Risks of Climate-Induced Disasters through Enhanced National and Local Capacity for Effective Actions*, funded by GEF-LDCF through UNDP and implemented by RGOB.

Report prepared by:
Yonten Phuntsho, Geologist

Reviewed by:
Ugyen Wangda, Chief Geologist
Tashi Tenzin, Project Manager, NAPA II Project, DGM

Suggested citation: Department of Geology and Mines (2018). *Monitoring of Landslide at Arong, Moshi and Phongmey using GPS.* Thimphu

Disclaimer

This publication has been produced with the assistance of the GEF-LDCF. The contents of this publication are the sole responsibility of Department of Geology and Mines, Ministry of Economic Affairs, Royal Government of Bhutan, and can in no way be taken to reflect the views of the GEF-LDCF and UNDP.

Comments and inquiries on this report can be emailed at: yphuntsho@moea.gov.bt or tashit@moea.gov.bt

དཔལ་ལྡན་འབྲུག་གཞུང་ བསྟན་རྒྱས་ལྷན་ཁག།
ས་རིག་དང་ས་གཏེར་ལས་ཁུངས་ ཐིམ་ཕུག།

Department of Geology and Mines
Ministry of Economic Affairs
Royal Government of Bhutan
Thimphu

Forward

Located in the eastern part of the Himalayas, the Kingdom of Bhutan is a small landlocked country between India and China. Being a part of young (ca. 55 million years) fold-thrust Himalayan mountain belt, more than 90 percent of the country's area is topographically rugged and geologically very fragile. In the foothills where rainfall is heavy during monsoon, the occurrence of landslides is significant. In recent years, landslide related risk to lives, livelihoods, infrastructures, properties and environment in the country is on rise because of intense and erratic rainfall pattern most likely induced by climate change and interactions of human activities with the nature.

Thus as an intervention to reduce risks associated with climate change induced landslide geohazard, the Department of Geology and Mines (DGM) under Ministry of Economic Affairs (MoEA), Royal Government of Bhutan (RGoB) has carried out the following two key activities under Outcome 1 and Output 1.3 of Second National Adaptation Programme of Action (NAPA-2) Project themed *'Addressing the Risks of Climate-Induced Disasters through Enhanced National and Local Capacity for Effective Actions*, funded by Least Developed Countries Fund (LDCF)-Global Environment Facility (GEF) through United Nations Development Programme (UNDP) and RGoB implementing partner National Environment Commission (NEC) between 2014 and 2017:

1. Integrated geohazard risk assessment and mapping of four critical landslide or landslide affected areas viz.: (1) Moshi landslides and (2) Arong/Lamsorong landslide on Samdrupjongkhar-Trashigang highway; (3) Box-cutting landslide on Gelephu-Zhemgang highway; and (4) Barsa watershed under Phuntsholing Dungkhag, Chukha Dzongkhag; and

2. Landslide monitoring and threshold development of six landslides namely: (1) Moshi landslide, (2) Arong/Lamsorong landslide, (3) Box-cutting landslide, (4) Tshimatsham

Tel: +975-02-322879,323096,323349,323409,324118, Fax: +975-02-323013,326134,324193,339845
P.O.Box No.173, Email:dgm@moea.gov.bt, URL:http://www.moea.gov.bt

དཔལ་ལྡན་འབྲུག་གཞུང་། བསྟན་རྒྱས་ལྷན་ཁག།
ས་རིག་དང་ས་གཏེར་ལས་ཁུངས་ ཐིམ་ཕུག།

Department of Geology and Mines
Ministry of Economic Affairs
Royal Government of Bhutan
Thimphu

on Phuentsholing-Thimphu highway under Chukha Dzongkhag, (5) Reldri landslide under Phuentsholing Thromdey, and (6) Lem landslide, Phongme Geog under Trashigang Dzongkhag.

The goal and objectives of these studies were to: (1) map and assess the four critical landslide affected areas using geo-scientific methods to provide findings and recommendations on suitable mitigation measures (both long term and short term); (2) monitor landslides using geoscientific methods to understand the movement behaviours and record landslide events; (3) develop rainfall thresholds for landslide initiation in the selected monitoring sites; (4) forecast or issue landslide warnings in regions with similar geological and topographical conditions through National Weather and Flood Forecasting and Warning Center (NWFFWC); and (5) share findings and recommendations of these studies with relevant users (national, district, local government, and others) for awareness and importantly for incorporation of the mitigation measures in their plans and implementations for reduction of risks associated with landslide geohazards.

In this regard, DGM on behalf of the Ministry and RGoB is pleased to publish the reports and maps for the four-critical landslide affected areas and six landslide monitoring sites in the country, whose findings and recommendations were shared to the relevant stakeholders during the two-day workshop held at Phuentsholing from 13-14, November 2017.

On behalf of the department, I acknowledge the effort put into publishing these reports and maps and I am hopeful that these documents will be useful to the relevant stakeholders who are responsible in dealing with risks associated with landslide in the study areas.

(Phuntsho Tobgay)
Director General

Tel: +975-02-322879,323096,323349,323409,324118, Fax: +975-02-323013,326134,324193,339845
P.O.Box No.173, Email:dgm@moea.gov.bt, URL:http://www.moea.gov.bt

ABSTRACT

Monitoring of landslide movement rate, particularly creep type of landslide, is important to understand the behaviour of the landslide and its threat to lives and properties. The information on landslide behaviours mainly displacement and rate of movement will help in timely decision making in dealing with the landslides to reduce risks. In this study, GPS monitoring of three critical landslides at Arong, Moshi and Phongmey in eastern Bhutan were carried out twice a year (pre-monsoon and post-monsoon) between August 2015 to May 2017.

The landslides at Arong and Moshi are located on one of the strategic national highways that connect Samdrujongkhar (a border town to India) to eastern districts like Pemagatshel, Trashigang, and Mongar. The landslide monitoring site at Phongmey is located about 30 km east of Trashigang town and poses threats to hundreds of lives and livelihoods of people under Phongmey Geog. Arong landslide falls within Diuri formation with rock mostly consisting of dark grey to green fine-grained phyllite and dark brown to black fine-grained slate. Moshi landslide falls within Shumar formation with rock mostly of light grey to light green to white fine-grained, medium to thick-bedded quartzite with thin to very thin grey black fine-grained phyllite interbeds. Phongmey landslide falls within Chekha formation comprising of schist with mica minerals like biotite and muscovite, quartz and garnet.

GPS monitoring of 6 control points in and around Arong landslide, 7 control points in and around Moshi landslide, and 6 control points in and around Phongmey landslide between August 2015 to May 2017 show all the monitoring control points in three landslides moved between each set of GPS observations with variable movements (displacement and rate). The total movement of control points is dominated by seasonal vertical movement compared to seasonal horizontal movement. The net average horizontal and vertical displacement for: (1) Arong is 0.25 m and 1.51 m respectively; (2) Moshi is 0.38 m and 0.66 m respectively; and (3) Phongmey is 0.08 m and 0.57 m respectively.

The net average velocity (movement rate) of 0.296 mm per day at Arong landslide falls under very slow to slow category of movement rate. The net average velocity (movement rate) of 0.150

mm per day at Moshi landslide and Phongmey landslide fall under the extremely slow category of movement rate. The net average movement rates of the Moshi and Phongmey landslides can be classified as stable movement and therefore indicate a normal situation. The net average movement rate of the Arong landslide can be classified as large seasonal fluctuations and therefore indicate an alert situation. However, since the GPS observations are made only on the surface or near-surface of the landslides with only few control points, therefore, monitoring using integrated monitoring systems approach (both contact and remote) that help determine more representative and accurate movement of these landslides is recommended. This will include but not limited to monitoring using instruments or techniques such as inclinometer, extensometer, piezometer, total stations, and satellite and terrestrial remote sensing.

All the 11 tension cracks in the three landslides also showed movement. The change in the length of the tension crack ranges from no movement for tension crack located in Moshi to 45.10 m for tension crack located in Arong landslide. Similarly, the change in the width of the tension crack ranges from 0.1 m for tension crack in Phongmey, Moshi and Arong to 0.4 m for tension crack in Phongmey.

Keywords: Landslide, Monitoring, Movement, GPS, Tension Cracks, Arong, Moshi, Phongmey.

TABLE OF CONTENTS

LIST OF FIGURES

LIST OF TABLES

ACRONYMS

BRO- Border Road Organization
GEF- Global Environment Fund
GIS- Geographic Information System
GPS- Geological Position System
LDCF- Least Developed Countries Fund
NAPA- National Adaptation Program of Action
NCHM- National Centre for Hydrology and Meteorology
UNESCO- United Nations Educational, Scientific and Cultural Organization

1. INTRODUCTION

Terzaghi (1950) defined landslide as a rapid displacement of a mass of rock, residual soil, or sediments adjoining a slope, in which the centre of gravity of the moving mass advances in a downward and outward direction and similarly the International Geotechnical Societies UNESCO working party on the World Landslide Inventory defined it as “The movement of a mass of rock, earth or debris down a slope” (Cruden, 1991 and Anon, 1997). Landslides are one of the major natural hazards, often causing property damage and other economic loss in terms of high reconstruction costs to the infrastructures such as highways, building etc. Landslides are triggered by different factors, both natural and anthropogenic (Althuwaynee and Pradhan, 2012).

Bhutan being a mountainous country, most landslides are found on cut slopes and the embankment of roads and highways. Landslides in Bhutan are mostly rainfall triggered and caused by anthropogenic activities blocking the highways, thereby threatening the life and property. Monitoring of landslide movement rate, particularly creep type of landslide, is important to understand the behaviour of the landslide and its threat to lives and properties. The information on landslide behaviours mainly displacement and rate of movement will help in timely decision making in dealing with the landslides to reduce risks.

Under the NAPA II project, six critical landslides were selected for monitoring. These landslides were selected based on the strategic location of the landslide and overall as a representative landslide to represent landslide in the country. This report is based on monitoring of three landslides at Arong, Moshi and Phongmey. Given the destructive nature of these landslides to property and economic loss, therefore monitoring of these landslides was undertaken.

1.1. AIM AND OBJECTIVES

The study in the above-mentioned landslide areas were carried out to understand the behaviour of each landslide based on the displacement (horizontal, vertical rate of movement) with respect to geographical location. This information on landslide behaviours mainly displacement and rate of movement will help in timely decision making in dealing with these landslides to reduce risks.

1.2. STUDY AREA

The locations of the three selected monitoring sites are shown in Figure 1.

Arong is located about 32 Km from Samdrupjongkhar- main shopping hub for the eastern region. The landslides fall right below the highway connecting Samdrupjongkhar to rest of the eastern region. This makes the road a lifeline for this region. The landslide is located at N 26.903° and E 91.505° with an elevation ranging from 1230 m to 1280 m. The landslide has the dimension of the length of 750 m and width of 350 m (Figure 2). The slide has undulating slope angles at a different location, but it has a general slope angle of 35° to 40° with the slide direction towards the North. The area usually has warm wet summer and cool dry winter. As per climate data of NCHM, the area received heaviest average monthly rainfall in June 2012 with 46.44 mm and similarly minimum monthly temperature was recorded in January 2005 with 6.7 °C and maximum monthly temperature of 27.76 °C in August 2007.

Moshi is located about 5 km from Wamrong town towards Samdrupjongkhar district. Similar to the Arong landslide, this landslide falls on the Samdrupjongkhar to Trashigang National highway. Hence this road too has the same importance as Arong. The landslide is location coordinate of N 27.112° and E 91.544° with the elevation ranging from 1740 to 1860 m. The area of the slide is about 700 m by 400 m (Figure 3). The general slope angle of the area ranges from 25° to 30° with slide direction towards north. The area usually has a wet summer season and dry winter season. As per climate data of NCHM, the area received the highest rainfall in the month of June 2012 with 46.44 mm. The minimum monthly temperature was recorded in January 2005 with 6.7 °C and maximum temperature was recorded in August 2007 with 27.76 °C.

Phongmey is located about 40km from Trashigang town and about 16km from Rangjung town. The landslide has the coordinate of N 27.371° and E 91.742° with elevation ranging from 1810 to 1860 m. The area of the slide is about 500m by 300m (Figure 4). The area usually has moderately wet summer season and dry cold winter season. As per climate data of NCHM, the area received the highest monthly rainfall in the month of August 2013 with 25.37 mm. Similarly, the minimum monthly temperature was recorded in January 2005 with 1.19 °C and maximum monthly temperature of 35.16 °C in August 2016.

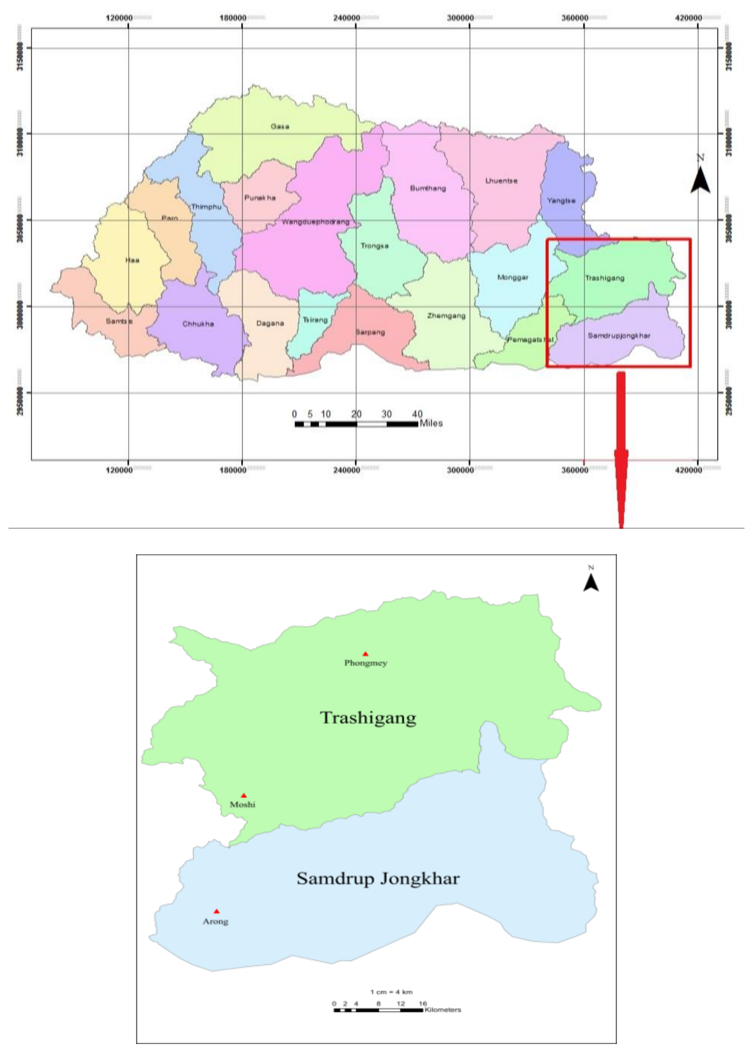

Figure 1. Location of the three selected landslide monitoring sites.

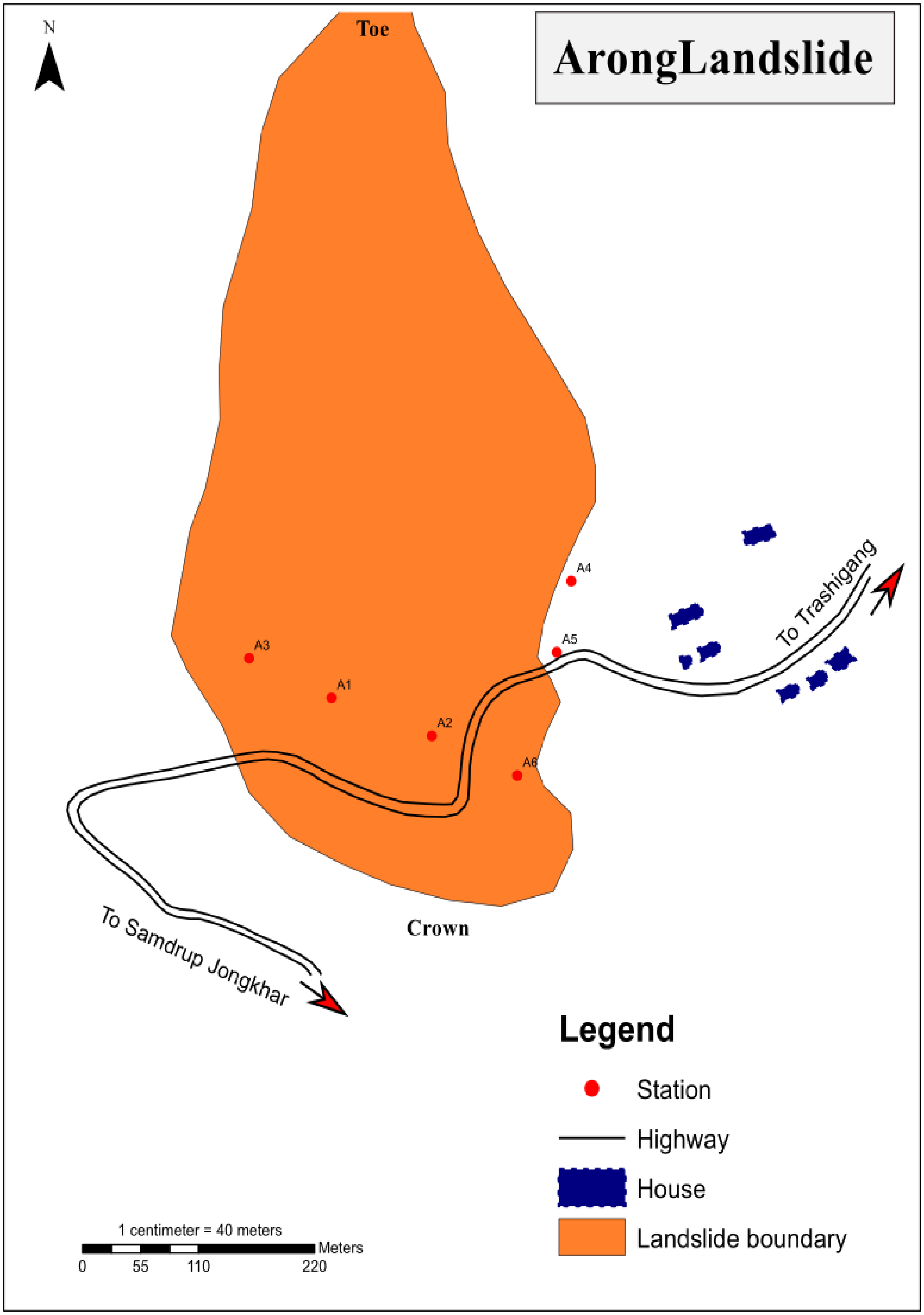

Figure 2. Arong landslide map showing prominent features and location of GPS observation points.

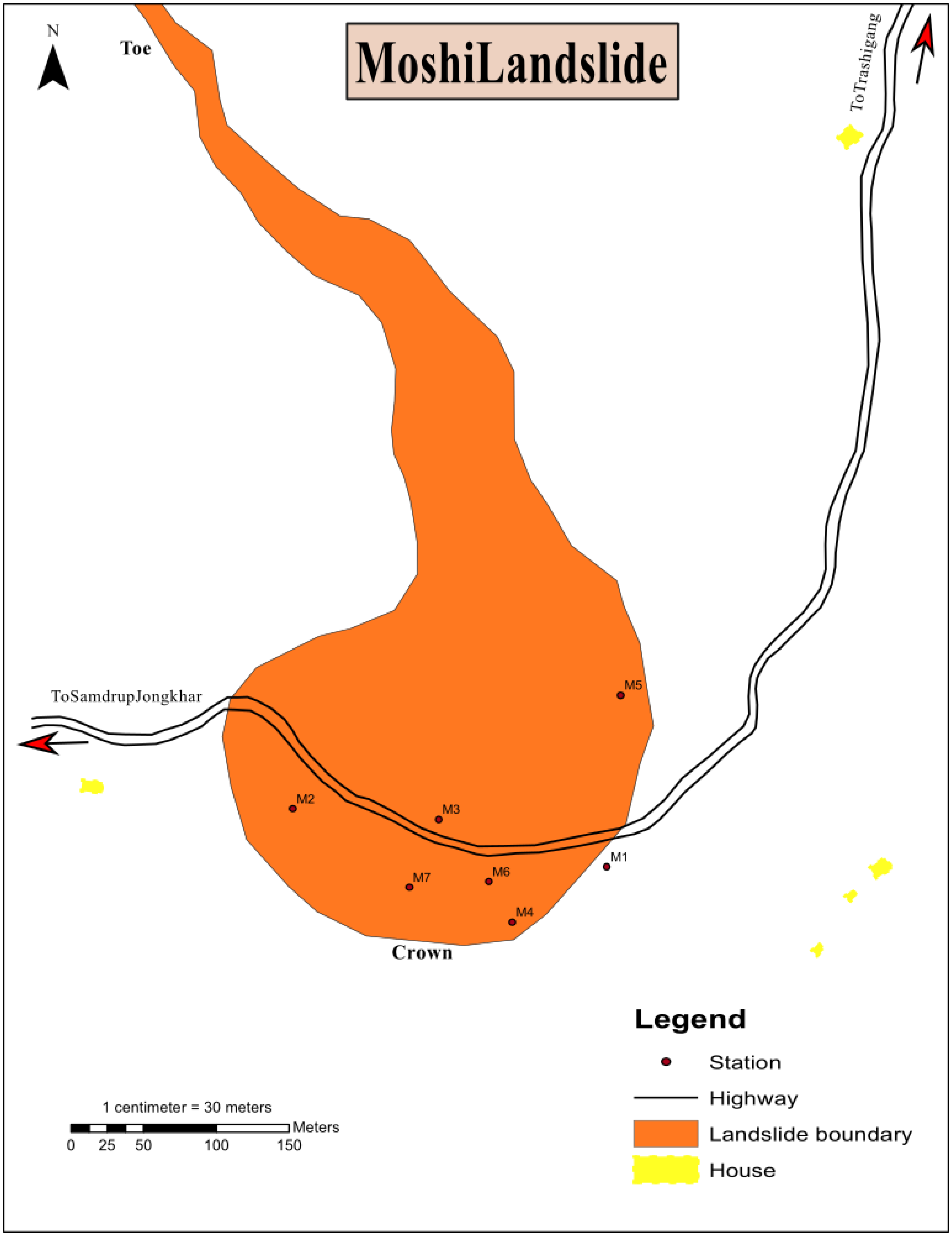

Figure 3. Moshi landslide map showing prominent feature along with the locations of GPS observation points

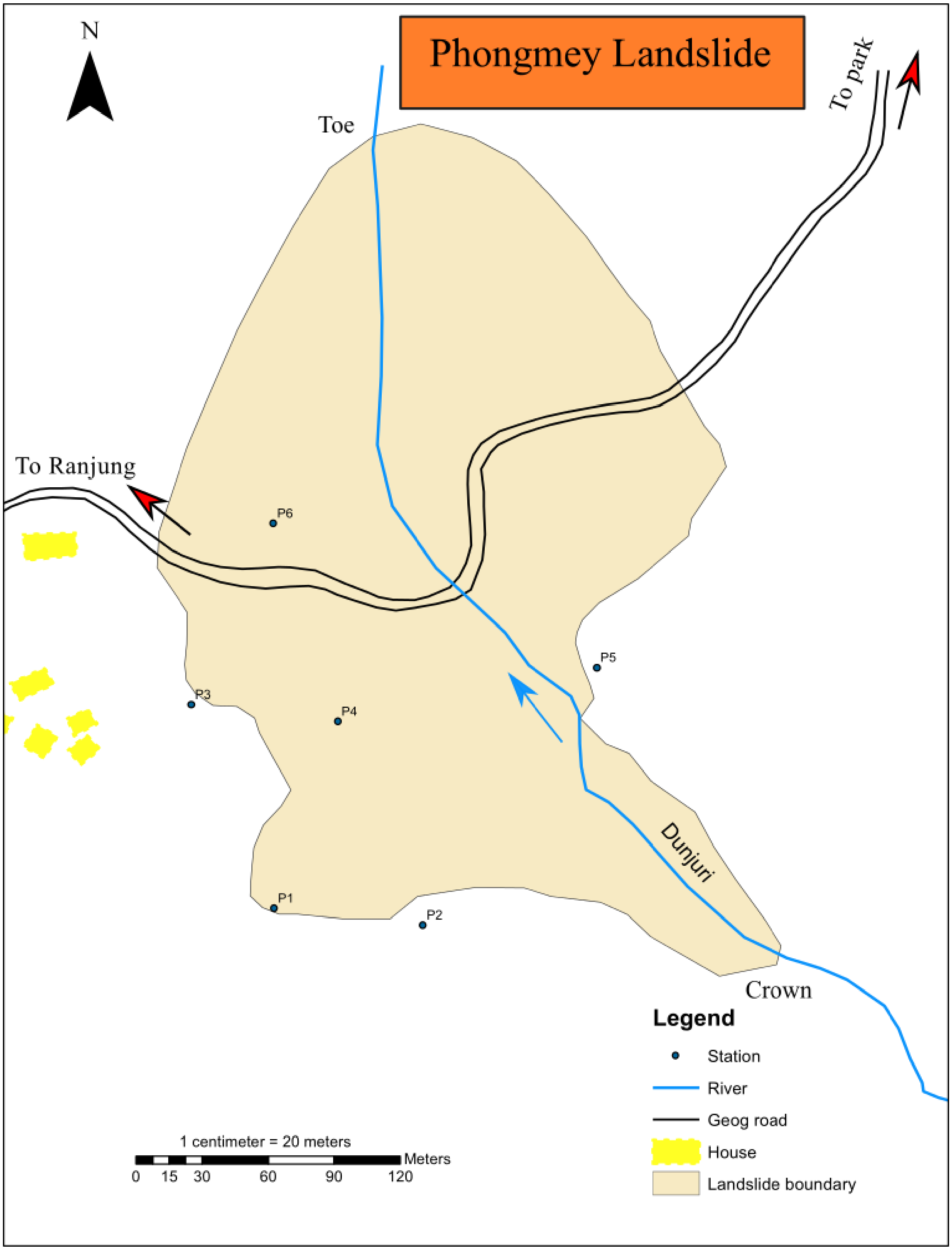

Figure 4. Landslide map of Phongmey with prominent features along with the location of GPS points.

2. GEOLOGY SETTING

2.1. Geological Setting of Arong Landslide

The area falls under the Diuri formation (Figure 5) with rock mostly consisting of dark grey to green fine-grained phyllite and dark brown to black fine-grained slate (McQuarrie et al., 2013; Long et al., 2011). The phyllite consists of minerals like chlorite and clayey materials. The rock generally dips 50° in the 45° NW directions. The grey and black slate have an irregular developed fracture and the rock is found to be dipping in the direction of slide, i.e. in the NW direction.

2.2. Geological Setting of Moshi Landslide

The area falls under Shumar formation (Figure 5) with rock mostly of light grey to light green to white fine-grained, medium to thick-bedded quartzite with thin to very thin grey black fine-grained phyllite interbeds (McQuarrie et al., 2013; Long et al., 2011). The average thickness of the quartzite is about 100 m. But the individual band of quartzite ranges from 10 cm to 2 m (Figure 5). The orientation of the rock is 48° NW with the average dip amount of 40° which is similar to the slope direction of the slide. The quartzite in the landslide area has undergone brittle deformation with many irregular joints.

2.3. Geological Setting of Phongmey Landslide

The area falls under Chekha formation (Figure 5). The majority of the rock observed is schist with mica minerals like biotite and muscovite, quartz and garnet (McQuarrie et al., 2013; Long et al., 2011). Fine grain quartzite is found as interband between the schist. The intrusion of black and white granite into the schist is also observed. The granite is coarse-grained with black amphibolite minerals, plagioclase and quartz. The rock in the area has a general orientation of 20° dip amount with 47° NW directions.

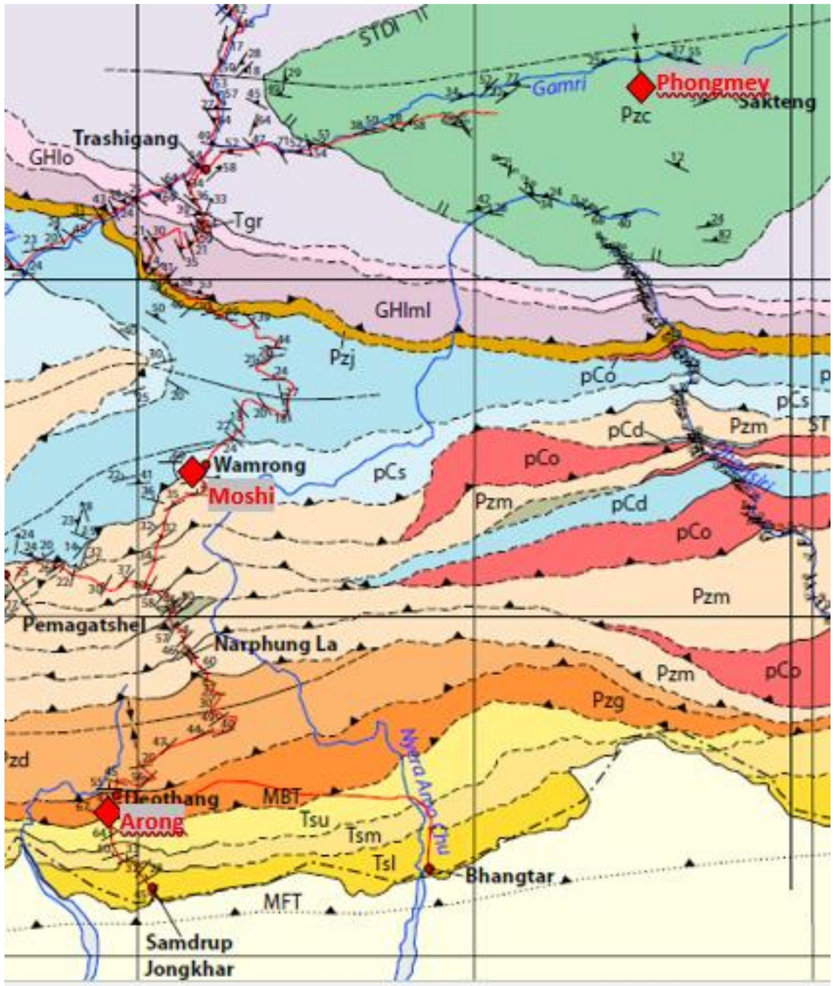

Lesser Himalayan Zone

Pzg — **Gondwana succession (Permian)** – Gray, medium-grained, feldspathic, lithic-rich sandstone interbedded with dark-gray to black, thin- to medium-bedded, carbonaceous siltstone, shale, slate, and argillite, and rare black coal beds (Gansser, 1983; Lakshminarayana, 1995; Long et al., 2011A). 1.2 to 2.4 km-thick (Long et al., 2011A).

Pzd — **Diuri Formation (Permian)** – Green-gray, pebble- to cobble-, slate-matrix diamictite (Gansser, 1983; Tangri, 1995b; Long et al., 2011A). Conglomerate at base along Kuri. 2.3 to 3.1 km-thick (Long et al., 2011A).

Pzj — **Jaishidanda Formation (Neoproterozoic-Ordovician[?])** – Gray, biotite-rich, locally garnet-bearing schist, interbedded with gray to tan, biotite lamination-bearing, lithic clast-rich quartzite (Bhargava, 1995; Dasgupta, 1995; Long et al., 2011A). Typically 600-900 m-thick, but 1,700 m-thick along Kuri (Long et al., 2011A). Upper greenschist to lower amphibolite facies (Gansser, 1983).

Daling-Shumar Group (Paleoproterozoic)

pCd — **Daling Formation** - Similar lithologies to Shumar Formation, but dominated by schist and phyllite. Quartzite is thin- to medium-bedded, and medium-gray limestone interbeds are rare. Lower contact is gradational with Shumar Formation (McQuarrie et al., 2008; Long et al., 2011A). Between 2.3 and 3.2 km-thick (Long et al., 2011A).

pCo — **Orthogneiss** - Concordant bodies of mylonitized, granitic orthogneiss at varying stratigraphic levels; interpreted as deformed Paleoproterozoic granite plutons that intruded Daling-Shumar Group (Long et al., 2011A). Thicker in easternmost Bhutan (Gansser, 1983). Interpreted as Indian crystalline basement east of Bhutan in Arunachal Pradesh (Yin et al., 2010).

pCs — **Shumar Formation** - Light-gray to white, tan-weathering, very fine-grained, medium- to thick-bedded, cliff-forming quartzite. Interbeds of thin- to thick-bedded, green, muscovite-biotite schist and phyllite with diagnostic sigmoidal quartz vein boudins become more common upsection. Between 1-2 km thick, except for 6 km-thick section local to Kuri valley (Long et al., 2011A). Upper greenschist facies (Gansser, 1983).

Figure 5. Location of the landslide on the Geological map of Bhutan by Long et al., (2011) showing the geological setting of the landslide monitoring sites at Arong, Moshi and Phongmey.

3. METHODOLOGY

The assessment of the three selected landslides behaviours were undertaken by means of monitoring scheme. The monitoring of the landslides was undertaken on the seasonal basis i.e. the field observation of the landslide was undertaken twice a year starting from August 2015 to May 2017 (Table 1). The first data observation was undertaken in August 2015 and 35 control points were installed around and on the landslides(Rawat et al., 2011). The control points were evenly distributed in stable areas around the periphery of the slide. The purpose of the control points is to monitor the seasonal movement of the slide using GPS(Coe & Lidke, 2003). At each control points, 2mm diameter rod with 1.5 feet was hammered into the ground for the GPS measurement (Figure 6B). The next observation was subsequently undertaken in May 2016 (7 months), September 2016 (4 months) and May 2017 (7months). The observation of the station points is given in Table 1.

Table 1. Date of observation of GPS points

Sl. No.	Seasonal Type	Date
1	Post-monitoring	21/08/15- 03/09/15
2	Pre-monitoring	28/05/16- 01/06/16
3	Post-monitoring	13/10/16- 18/10/16
4	Pre-monitoring	23-05-17 - 04/06/17

The map of the landslide area and the horizontal movement between the previous monitoring points of the landslide area was prepared using ArcGIS version 10.4.1. The conversion of coordinates of the monitoring points from one coordinate to another was done using Lat-Long converter software. The digitization of features like road, landslide boundary and houses were done on georeferenced google earth image as a base map by ArcGIS version 10.4.1. The google earth image is geo-referenced using Elshayal

Smartgis. Along with the GPS observation of the crack found on the landslide areas, change in the dimension of the crack was measured using tapes and wire method (Table 3). The post-processing of the observation data of the GPS was done with the help of Natural Resource Canada. The observation data in the RINEX format was sent to Natural Resource Canada through online on the processed data was received through the registered email.

3.1. GPS Method

The following GPS surveying is based on the seasonal movement of the Slumgullion landslide as determined from GPS observation, July 1998-July 1999(Coe & Lidke, 2003)(Anon, 2000). The primary task of GPS surveying is to measure the distance between the satellite and the location of the earth (Figure 6A). Once the distance has been measured, coordinates of positions on the earth are calculated by triangulation. Distances are measured based on the amount of time required for an electromagnetic GPS signal to travel from the satellites to ground-based antennas and receivers. Antennas collect the satellite signal and convert the electromagnetic waves into electric currents that can be recorded by the receiver (Rawat et al., 2011).

Satellites transmit precise time and location information in three binary codes, precise code, coarse and acquisition code and navigation code. The codes are transmitted on two carrier waves that are part of the L-band of the microwave electromagnetic spectrum. The two carrier waves have frequencies called L1 and L2.

There are two main GPS surveying methods, kinematic and static surveying. In kinematic applications, receivers are in motion during the measurement period and real-time positioning solution is available based on the pseudo-range observables in static applications, receivers are stationary for long measurements periods (generally >30minutes) and both pseudo-range and carrier phase data are post-processed for precise positioning solutions. Rapid static applications are the same as static techniques except that occupation times are short, generally from 5 to 20 minutes, and post-processing relies on code and L1 and L2 carrier phase observations.

The type and accuracy of positioning in kinematic and static surveying is dependent on the number of receivers available. There are two types of positioning, single points and relative. Single-points positioning is the determination of a ground position using one receiver and observables from one or more satellites. Single-points positioning relies on the pseudo-range observable. The accuracy of the single-points positioning increases with the number of satellites available. Relative positioning is the determination of a ground position using two or more receivers and two or more satellites. Relative positioning allows for the elimination of clock and atmospheric errors in the carrier-phase signal by combining simultaneous observables (referred to as differencing in GPS terminology) from multiple receivers and satellites during post-processing. Relative positioning determines the precise vector (baseline) between receiver positions. When the coordinates of one of the receiver positions is known, that receiver is referred to as a base station, and the known coordinates and baseline can be used to determine the precise coordinates of the unknown points.

Figure 6. A) GPS used for the observation of points at Arong. B) 60 cm rod used to mark the GPS station points with a geological hammer for scale.

In relative positioning, data is stored in the receivers and is post-processed using computer software to calculate baselines, determine unknown coordinate positions, and estimate horizontal and vertical errors for calculated positions. If baselines are calculated from two or more base stations, the baselines and coordinates of unknown points can be further refined through the use of a least-squares adjustment performed by holding the base station positions fixed while adjusting the baselines and coordinate positions of the unknown positions.

A requirement of relative positioning is that the receivers are capable of recording at least one of the carrier phases. Although many types of receivers are available, dual-frequency receivers are commonly used for relative positioning because they record all GPS codes, as well as the L1 and L2 carrier phases. In addition to recording all components of the GPS signal, dual frequency receivers generally have 12 channels, which allow them to simultaneously record the signals of up to 12 satellites.

4. FIELD OBSERVATIONS

4.1. CONTROL POINTS

Dates of observation, coordinates, height and positional errors for all 19 monitoring points are given in Table 2. Positional errors are given as standards errors and are always less than 2 cm for both horizontal and vertical points.

4.2. MOVEMENTS AND VELOCITIES OF MONITORING POINTS

The seasonal horizontal and vertical movement as compared with the previous points and seasonal velocity is given in Table 3 (Coe & Lidke 2003).

Table 2. Positions of monitoring points for each GPS observation along with the standard error for easting, northing and elevation (Coe and Lidke, 2003; Anon 2000)

Station	Date of GPS observation	Easting(m)	Standard Error of Easting value	Northing(m)	Standard Error of Northing value(m)	Elevation (m)	Standard Error of Elevation value(m)	Days since previous observation
A1	21-08-2015	351463.001	±0.011	2976370.089	±0.005	1248.192	±0.036	N.A
A1	02-06-2016	351463.026	±0.004	2976370.138	±0.001	1247.873	±0.006	286
A1	13-10-2016	351463.003	0.008	2976370.083	0.035	1248.193	0.0032	133
A1	05-06-2017	351463.112	±0.013	2976370.208	±0.005	1246.369	±0.027	235
M1	27-08-2015	355866.987	±0.013	2999625.023	±0.005	1855.132	±0.032	N.A
M1	28-05-2016	355866.982	±0.006	299625.053	±0.003	1854.743	±0.015	275
M1	27-05-2017	355867.035	±0.012	2999625.118	±0.004	1853.485	±0.023	364
P1	01-09-2015	375562.141	±0.013	3028047.459	±0.007	1859.451	±0.047	
P1	29-10-2016	375562.141	0.0117	3028047.458	0.006	1859.449	0.0165	424
P1	23-05-2017	375563.106	±0.014	3028047.763	±0.004	1857.745	±0.022	206
A2	04-04-2016	351552.325	±0.005	2976338.002	±0.001	1244.81	±0.008	
A2	05-05-2016	351552.319	±0.003	2976338.006	±0.001	1244.823	±0.005	397
A2	14-10-2016	351552.356	0.0091	2976337.883	0.006	1245.083	0.02	162
A2	04-06-2017	351552.238	±0.016	2976338.17	±0.005	1243.167	±0.022	233
M2	28-08-2015	355665.268	±0.016	2999663.299	±0.009	1868.698	±0.045	
P2	01-09-2015	375626.312	±0.011	3028040.225	±0.006	1863.86	±0.045	
P2	29-10-2016	375626.313	0.051	3028040.224	0.046	1863.86	0.03	424

P2	23-05-2017	375626.36	±0.013	3028040.314	±0.003	1862.186	±0.035	206
M3	28-08-2015	355758.93	±0.011	2999656.373	±0.006	1835.56	±0.038	
M3	30-05-2017	355759.145	±0.013	2999657.746	±0.003	1832.77	±0.034	641
P3	02-09-2015	375526.529	±0.012	3028136.532	±0.007	1826.975	±0.048	
P3	30-05-2016	375526.546	±0.005	3028136.581	±0.003	1826.596	±0.011	271
P3	30-10-2016	375526.528	0.0051	3028136.533	0.046	1826.973	0.0253	153
P3	24-05-2017	375543.755	±0.015	3028130.222	±0.004	1826.159	±0.029	206
A4	23-08-2015	351676.561	±0.011	2976468.971	±0.006	1231.946	±0.036	
A4	06-06-2017	351706.295	±0.016	2976439.964	±0.006	1239.909	±0.032	
M4	29-08-2015	355806.356	±0.013	2999588.256	±0.007	1875.003	±0.038	
M4	28-05-2016	355806.384	±0.004	2999588.281	±0.002	1874.351	±0.008	273
P4	24-05-2017	375584.008	±0.013	3028133.351	±0.005	1814.728	±0.027	
P4	02-09-2015	375589.602	±0.014	3028129.202	±0.009	1815.368	±0.056	
A5	24-08-2015	351663.652	±0.013	2976408.779	±0.006	1257.556	±0.034	
A5	05-05-2016	351663.574	±0.004	2976408.937	±0.001	1257.164	±0.006	255
A5	17-10-2016	351663.653	0.0051	2976408.777	0.051	1257.555	0.0253	165
A5	04-06-2017	351663.433	±0.012	2976409.173	±0.006	1255.463	±0.027	230
M5	29-08-2015	355875.986	±0.082	2999738.679	±0.021	1799.715	±0.163	
M5	01-06-2017	355876.085	±0.063	2999738.669	±0.022	1798.121	±0.155	642
P5	03-09-2015	375701.015	±0.011	3028152.688	±0.006	1841.528	±0.045	
P5	30-05-2016	375701.032	±0.004	3028152.716	±0.001	1741.299	±0.007	270
P5	25-05-2017	375701.063	±0.015	3028152.753	±0.004	1839.773	±0.022	360

A6	24-08-2015	351628.454	±0.012	2976304.505	±0.005	1282.565	±0.034	
A6	04-04-2016	351628.408	±0.004	2976304.614	±0.001	1282.083	±0.007	224
A6	18-10-2016	351628.453	0.0051	2976304.507	0.046	1282.564	0.003	197
A6	06-06-2017	351628.349	±0.013	2976304.759	±0.004	1280.449	±0.02	231
M6	29-08-2015	355791.257	±0.022	29999615.11	±0.006	1855.461	±0.044	
M6	28-05-2016	355791.255	±0.011	2999615.395	±0.004	1854.675	±0.012	273
P6	30-05-2016	375561.783	±0.006	3028215.716	±0.002	1783.995	±0.008	
P6	25-05-2017	375560.825	±0.015	3028216.433	±0.004	1782.249	±0.026	360
M7	27-08-2015	355740.151	±0.014	2999611.314	±0.006	1862.355	±0.035	
M7	28-05-2017	355740.269	±0.011	2999611.956	±0.004	1859.85	±0.022	640

Table 3. Summary of movements, the direction of movements, and velocities of monitoring points (Coe & Lidke, 2003; Anon 2000).

Station	Date of GPS observation	Easting	Northing	Elevation	Seasonal horizontal movement (m, from previous position)	Seasonal horizontal velocity (m/day, since previous position)	Seasonal horizontal movement direction	Annual horizontal movement (m, net from 21/8/15 to 6/6/17	Seasonal vertical movement (m, from previous position)	Seasonal vertical velocity (m/day, since the previous position)	Annual vertical movement (m, net from 21/8/15 to 6/6/17	Days since previous observation
A1	21.8.15	351463.001	2976370.089	1248.192								N.A
A1	2.4.16	351463.026	2976370.138	1247.873	0.0550	0.0001923	NE		0.319	0.001115		286
A1	13.10.16	351463.003	2976370.083	1248.193	0.0596	0.0004481	SE		-0.320	0.002406		133
A1	5.6.17	351463.112	2976370.208	1246.369	0.1658	0.0007055	NE	0.16	1.824	0.007761	1.823	235
M1	27.8.15	355866.987	2999625.023	1855.132								N.A
M1	28.5.16	355866.982	2999625.053	1854.743	0.0300	0.0001090	NW		0.389	0.001414		275
M1	27.5.17	355867.035	2999625.118	1853.485	0.0840	0.0002307	NE	0.10	1.258	0.003456	1.647	364
P1	1.9.15	375562.141	3028047.459	1859.451								N.A
P1	29.10.16	375562.141	3028047.458	1859.449	0.001	0.0000023	NS		0.002	4.71698E		424
P1	23.5.17	375563.106	3028047.763	1858.745	1.0118	0.0049116	NE	1.01	0.706	0.003427	0.706	206
A2	22/8/201	351552.325	2976338.002	1244.810								N.A
A2	5.4.16	351552.319	2976338.006	1244.823	0.0072	0.0000181	NW		-0.013	3.27456E		397
A2	14.10.16	351552.356	2976337.883	1245.083	0.1284	0.0007925	SE		-0.26	0.001604		162
A2	4.6.17	351552.238	2976338.170	1243.167	0.1830	0.0007854	NW	0.18	1.656	0.007107	1.643	233

P2	1.9.15	375626.312	3028040.225	1863.86									N.A
P2	29.10.16	375626.313	3028040.224	1863.86	0.0014	0.0000033	SE		0	0			424
P2	23.5.17	375626.360	3028040.314	1863.186	0.1011	0.0004907	NE	0.10	0.674	0.003271		0.674	206
A3	23.8.15	351389.317	2976403.565	1263.087									N.A
A3	2.4.16	351389.369	2976403.586	1262.722	0.0561	0.0002217	NE		0.365	0.001442			253
A3	15.10.16	351389.316	2976403.565	1263.085	0.0561	0.0003379	SW		-0.363	0.002186			166
A3	5.6.17	351389.461	2976403.631	1261.235	0.1020	0.0004377	NE	0.15	1.487	0.006381			233
M3	28.8.15	355758.93	2999656.373	1835.56									
M3	30.5.17	355759.145	2999657.746	1834.77	1.3890		NE	1.38	0.79	0.001232			641
P3	2.9.15	375526.529	3028136.532	1826.975									N.A
P3	30.5.16	375526.546	3028136.581	1826.596	0.0519	0.0001915	NE	0.05	0.379	0.001398			271
P3	30.10.16	375526.528	3028136.533	1826.973	0.0512	0.0003350	SW		-0.377	-		0.379	153
A4	23.8.15	351676.561	2976468.971	1231.946									
A4	6.6.17	351706.295	2976439.964	1239.909									
M4	29.8.15	355806.356	2999588.256	1875.003									N.A
M4	28.5.16	355806.384	2999588.281	1874.351	0.0375	0.0001373	NE	0.03	0.652	0.002388		0.652	273
P4	2.9.15	375589.602	3028129.202	1815.368									
P4	24.5.17	375584.008	3028133.351	1814.728	6.9650								
A5	24.8.15	351663.652	2976408.779	1257.556									N.A
A5	5.4.16	351663.574	2976408.937	1257.164	0.1760	0.0006901	NW		0.392	0.001537			255

A5	17.10.16	351663.653	2976408.777	1257.555	0.1760	0.0010666	SE		-0.391	0.002369		165
A5	4.6.17	351663.433	2976409.173	1255.463	0.4530	0.0019695	NW	0.45	1.701	0.007395	2.093	230
M5	29.8.15	355875.986	2999738.679	1799.715								N.A
M5	1.6.17	355876.085	2999738.669	1799.121	0.0995	0.0001549	EW		0.594	0.000925	0.594	642
P5	3.9.15	375701.015	3028152.688	1841.528								N.A
P5	30.5.16	375701.032	3028152.716	1841.299	0.0328	0.0001214	NE		0.229	0.000848		270
P5	25.5.17	375701.063	3028152.753	1840.773	0.0483	0.0001341	NE	0.08	0.526	0.001461	0.755	360
A6	24.8.15	351628.454	2976304.505	1282.565								N.A
A6	4.4.16	351628.408	2976304.614	1282.083	0.1180	0.0005267	NW		0.482	0.002151		224
A6	18.10.16	351628.453	2976304.507	1282.564	0.1161	0.0005893	SE		-0.481	-		197
A6	6.6.17	351628.349	2976304.759	1281.449	0.2725	0.0011796	NW	0.27	0.634	0.002744	1.116	231
M6	29.8.15	355791.257	2999615.112	1855.461								N.A
M6	28.5.16	355791.255	2999615.395	1854.675	0.2830	0.0010366	SN	0.28	0.786	0.002879	0.786	273
P6	30.5.16	375561.783	3028215.716	1783.995								N.A
P6	25.5.17	375560.825	3028216.433	1783.249	1.1970	0.0033250	NW	1.19	0.746	0.002072	0.746	360
M7	27.8.15	355740.151	2999611.314	1862.355								N.A
M7	28.5.17	355740.269	2999611.956	1861.85	0.6530	0.0010203	NE	0.65	0.505	0.000789	0.505	640

Table 4. Summary of movements of tension cracks in the three monitoring sites.

Tension Cracks in Arong.

S.I No.	Easting	Northing	Elevation	Dimension of tension crack in August 2015 (m)	Dimension of tension crack in May 2016 (m)	dM	Dimension of tension crack in May 2017 (m)	dM	Remarks
1	351546	2976323	1299	L=13.30	Whole tension crack wash away (date unknown)		L=5		below the road
				W=1			W=0.4		
2	351667	2976409	1293	L=32.40	blacktop		122.5	45.1	the tension crack has merged on the fencing and road
				W=0.305					
3	351609	2976394	1283	L=45	blacktop		W= 0.45	0.15	
				W=0.08					
4	351526	2976279	1295	L=30	The crack cannot be determined due to blacktopping in the tension cracks.		L=43	13	road
				W=0.40			D=0.50	0.1	
5	351523	2976280	1280	L=10.6	L=13m	2.4	L=15	2	in the farm
				W=1.0	W=1.5	0.5	W=2.3	0.8	

Tension Cracks in Moshi

S.I No.	Easting	Northing	Elevation	Dimension of tension crack in August 2015 (m)	Dimension of tension crack in May 2016 (m)	dM	Dimension of tension crack in May 2017 (m)	dM	Remarks
1	355803	2999638	1887	L=15	covered with soil		covered with soil		On the road
				W=0.05					
2	*352135*	*2976570*	*1856*	*L=45*	*the tension crack*		*the tension crack*		*on the road*
				W=0.2					
3	*355698*	*2999631*	*1892*	*L=5*	*L=5*	*0*	*L=7*	*2*	*above the road*
				W=0.1	*D=0.2*	*0.1*	*0.3*	*0.1*	

Tension cracks in Phongmey.

S.I no	Easting	Northing	Elevation	Dimension of tension crack in August 2015 (m)	Dimension of tension crack in May 2016 (m)	dM	Dimension of tension crack in May 2017 (m)	dM	Remarks
1	375621	3028039	1901	L=15	L=18	3	41	23	crack near the house
				W=0.30	w=0.37	0.07	0.42	0.79	
2	375566	3028057	1894	L=3	L=5	2	12.5	7.5	crack near the chili garden
				W=0.4	w=0.5	0.1	0.9	0.4	
3	375587	3028065	1293	L=32.40	covered		covered		crack on the road
				W=0.31					

5. RESULTS AND DISCUSSIONS

The results for the observations of the data of the landslides are divided into two sections: (1) Movement of GPS points, and (2) Tension cracks.

5.1. Movement of GPS Points

5.1.1. Arong Landslide

Graph showing the rate of movement of control points at Arong landslide is shown in Figure 7. In Arong landslide all the observation points have moved the maximum (compared with the previous observation) from 13/10/16 to 6/6/17 i.e. during the fourth observation. The maximum movement is observed in points A5 with the horizontal movement of 0.4530 m during 17/10/15 to 4/6/17 and minimum horizontal movement of 0.0072 observed in points A2 during 22/8/15 to 5/4/16. In terms of velocity per day, the points A5 has the maximum horizontal velocity of 0.001969 m/d and A2 has the minimum velocity of 0.00001813 m/d (Table 3).

Table 5. Description of the rate of movement of the landslide.

Rate description	Varnes (1978) rate/period	WP/WLI (1995) millimetre/second
extremely rapid	>3metres/second	> 5 by 10^3
very rapid	>0.3 metres/minute	> 50
rapid	>62.5 millimetres/hour	> 0.5
moderate	>50 millimetres/day	> 5 by 10^{-3}
slow	>4.1 millimetres/day	> 0 by 10^{-3}
very slow	>0.164 millimetres/day	> 50 by 10^{-3}
extremely slow	<0.164 millimetres/day	< 0.5 by 10^{-3}

Similarly, the maximum vertical movement is observed in points A5 with the vertical movement of 1.7m between 17/10/16 and 4/6/17 and minimum of 0.013 m observed in points A2 from 22/8/15 to 14/10/16. In terms of velocity per day, the points A5 has the maximum vertical velocity of 0.00739m/d from 17/10/16 to 4/6/17 and points A2 from 5/4/16 to 14/10/16 has the minimum of all the points in Arong with 0.00003275m/d (Table 3).

In term of annual horizontal movement from 21/8/15 to 6/6/17 points, A5 has the maximum value of 0.453 m and points A3 has the minimum value of 0.1584m (Table 3). Similarly, in term of annual vertical movement from 21/8/15 to 6/6/17points A5 has the maximum value with 2.093m and points A1 has the minimum value of 0.823m (Table 3).

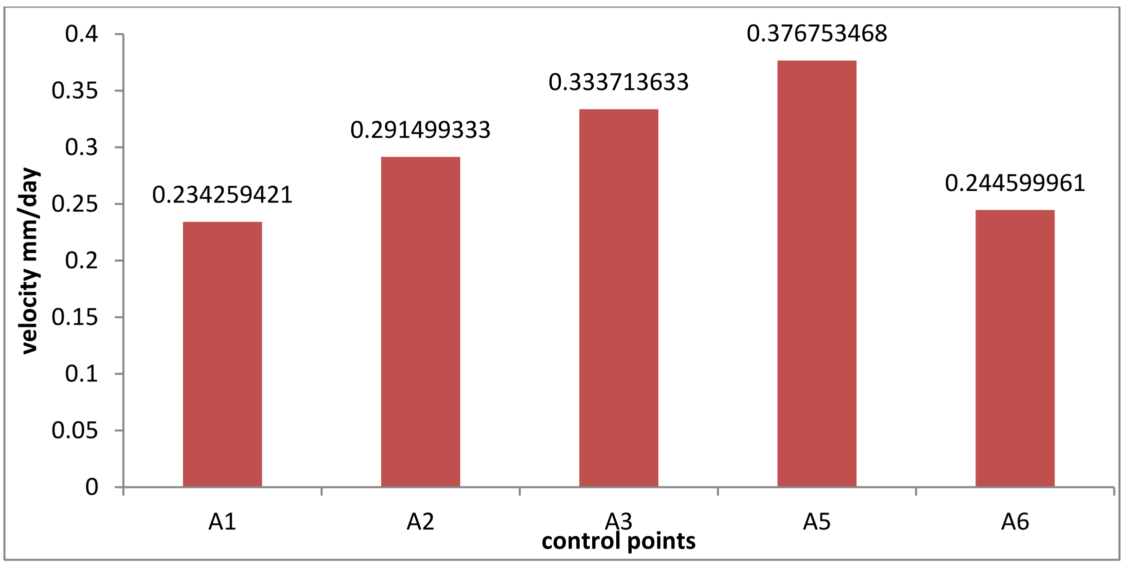

Figure 7. Graph showing the rate of movement of control points at Arong landslide

After comparing all the GPS points in Arong landslide from Table 3, in term of annual horizontal movement, it is observed that the eastern part of the landslide (A5, A6) shows greater movement as compared to central (A2) and western part of the landslide. The western part shows the minimum movement (A1, A3). Similarly, in terms of annual vertical movement the result is random as all the region of the landslide show similar vertical movement, hence the maximum and minimum movement in term vertical cannot be determined. The velocity of the control points in the mm/day (Figure 7) is correlated with the description of the movement of the landslide (Table 5). The horizontal velocity of all the points is <0.376 mm per day and therefore fall under very slow to slow category of movement rate as per classification of Varnes (1978).

5.1.2. Moshi Landslide

Graph showing the rate of movement of control points at Moshi landslide is shown in Figure 8. At Moshi landslide, 7 observation points have been used for observation of horizontal and vertical movement. The maximum horizontal movement of 1.389 m is observed in points M3 between 28/8/15 to 30/5/17 and minimum horizontal movement of 0.03 m is observed in points M1 between 27/8/15 to 28/5/16. In term of velocity in the horizontal movement of the points, M3 has the maximum horizontal velocity with 0.00217m/d and points M1 has the minimum velocity with 0.0001091m/d (Table 3).

Similarly, the maximum vertical movement is observed in points M1 with the vertical movement of 1.258m between 28/5/16 to 27/5/17 and a minimum of 0.389 m also observed in points M1 from 27/8/15 to 28/5/16. In terms of velocity the points M1 has the maximum vertical velocity of 0.0034m/d from 28/5/16 to 28/5/17 and points M7 from 27/8/15 to 28/5/17 has the minimum vertical movement of all the points in Moshi with 0.000789m/d (Table 3).

In term of annual horizontal movement from 21/8/15 to 6/6/17 point, M3 has the maximum value of 1.389m and points M4 has the minimum value with 0.0375m (Table 3). Similarly in term of annual vertical movement from 21/8/15 to 6/6/17points M1 has the maximum value with 1.647m and points M7 has the minimum value of 0.505m (Table 3).

After comparing all the GPS points in Moshi landslide from Table 3, in term of annual horizontal movement, it is observed that the central part of the landslide (M3, M7) shows greater movement as compared to eastern (M1) part of the landslide. The movement of western could not be compared due to the huge deviation of the data. Similarly, in terms of annual vertical movement, the result is random as all the region of the landslide show similar vertical movement, hence the maximum and minimum movement in term vertical cannot be determined.

The velocity of the control points in the mm/day (Figure 8) is correlated with the description of the movement of the landslide (Table 5). The horizontal velocity of all the points is <0.288 mm per day and therefore fall under very slow to slow category as per classification of Varnes (1978).

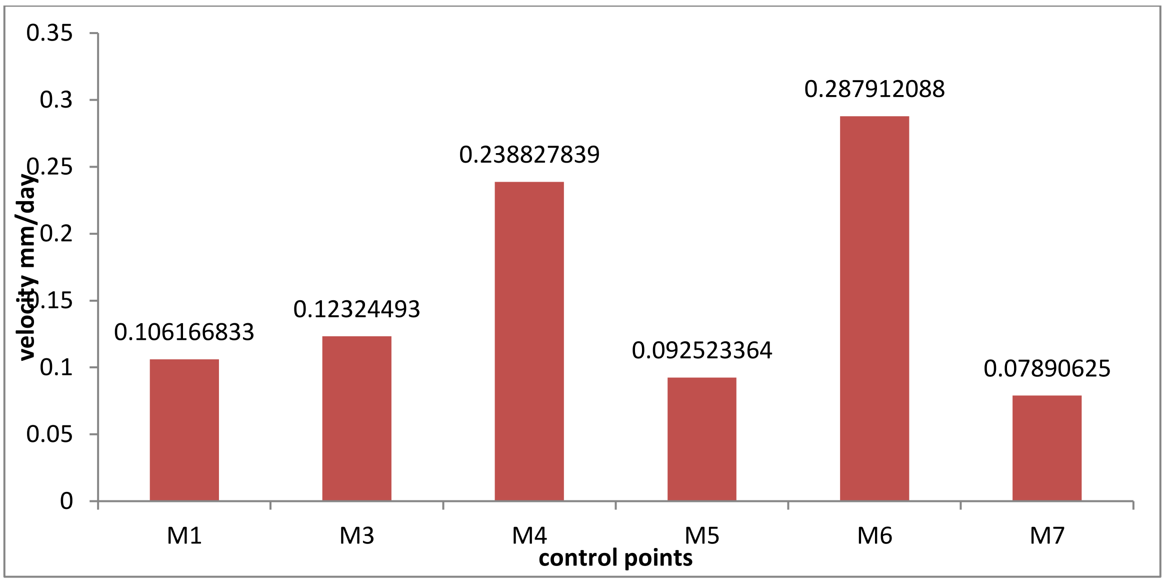

Figure 8. Graph showing the rate of movement of control points at Moshi landslide.

5.1.3. Phongmey Landslide

Graph showing the rate of movement of control points at Phongmey landslide is shown in Figure 9. At Phongmey landslide out of 6 observation points, only 5 observations have been used for observation of horizontal and vertical movement due to inconsistent data for points P4. The maximum horizontal movement of 1.197 m is observed in points P6 between 30/5/16 to 25/5/17 and minimum horizontal movement of 0.0001 m is observed in points P1 between 1/9/15 to 29/10/16. In term of velocity in the horizontal movement of the points, P1 has the maximum horizontal velocity with 0.00491m/d and points P1 has the minimum velocity with 0.000002358m/d (Table 3).

Similarly, the maximum vertical movement is observed in points P6 with the vertical movement of 0.746m between 30/5/16 to 25/5/17 and a minimum of 0m observed in points P2 from 1/9/15 to 29/9/16. In terms of velocity per day the points P1 has the maximum vertical velocity of 0.0034m/d from 29/10/16 to 23/5/17 and points P2 during 1/9/15 to 29/10/16 has the minimum of all the points in Phongmey with 0m/d (Table 3).

In term of annual horizontal movement from 21/8/15 to 6/6/17 points, P6 has the maximum value of 1.197m and points P3 has the minimum value of 0.0519m (Table 3). Similarly, in term of annual vertical movement from 21/8/15 to 6/6/17 P5 has the maximum vertical movement with 0.755m and points P3 has the minimum vertical movement with 0.379 (Table 3).

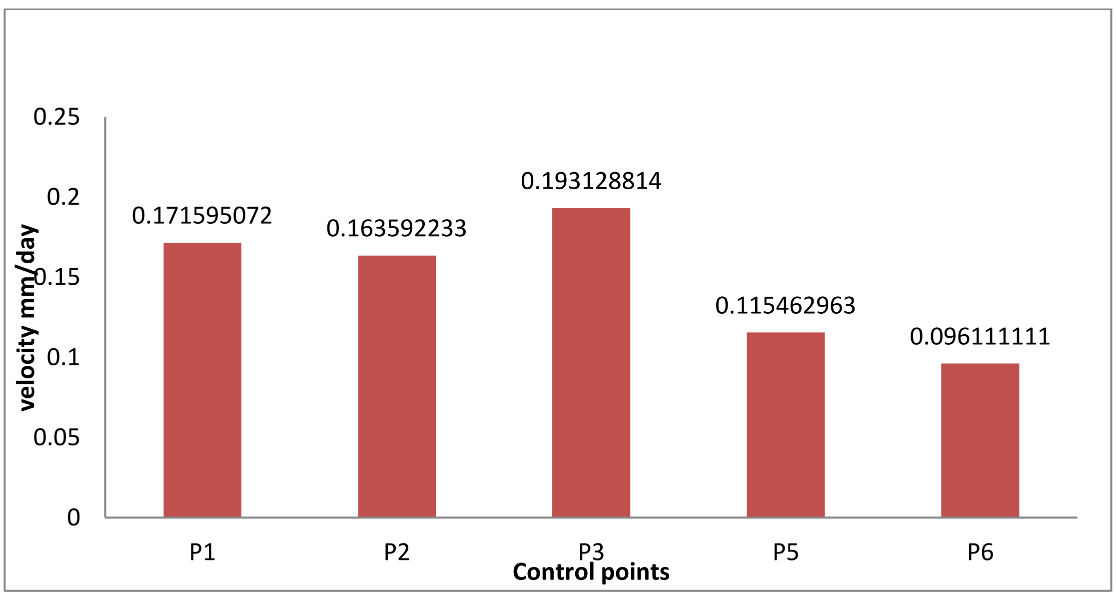

Figure 9. Graph showing the rate of movement of control points at the Phongmey landslide.

After comparing all the GPS points in Phongmey landslide from Table 3, in term of annual horizontal movement, it is observed that the western part of the landslide (P6, P1) shows greater movement as compared to western (P5) part of the landslide. Similarly, in terms of annual vertical movement, the result is random as all the region of the landslide shows a similar amount of vertical movement, hence the maximum and minimum movement in term vertical cannot be determined.

The velocity of the control points in the mm/day (Figure 9) is correlated with the description of the movement of the landslide (Table 5). The horizontal velocity of all the points is < 0.193 mm per day and therefore fall under extremely slow to slow category as per classification of Varnes (1978).

.

Figure 10. Depression/subsidence of land at Phongmey. The sinking of land has increased the height of the fencing. The book shows the height of fencing in the past.

5.2. Tension Cracks

While monitoring the landslide about 11 major tension cracks has been monitored using the measuring tape. The data of the tension crack and the GPS survey of the control points were collected during the same duration. The observation of measurement of the tension cracks has been given in Table 4.

5.2.1. Arong Landslide

During the first observation at Arong on August 2015, a tension crack with coordinate E 91.5051 and N 26.90078 and dimension 13.30m length and 1m width was observed and measured. However, during the second observation in May 2016, the same tension crack has been washed away (Figure 11). Similarly, the tension crack observed on the road with coordinate N 26.9015° and E 91.50633° during the first observation has been blacktop during the second observation. Therefore, the tension crack could not be measured (Figure 12).

The tension crack on the road has propagated during the observation on May 2017. During the site visit, it was found that the two-tension crack measured on the road during the first field visit has merged and has become one. The combined dimension was observed as 122.5m length by 0.45m width. The deviation of 45.1m in length and 0.145m in width was noted (Table 4).

The tension crack in the farm with coordinate N 26.90039 and E 91.50491 has the deviation of 2.4 m in length and 0.5m in width during May 2016 and 2m in length and 0.8m in width in May 2017 (Table 4).

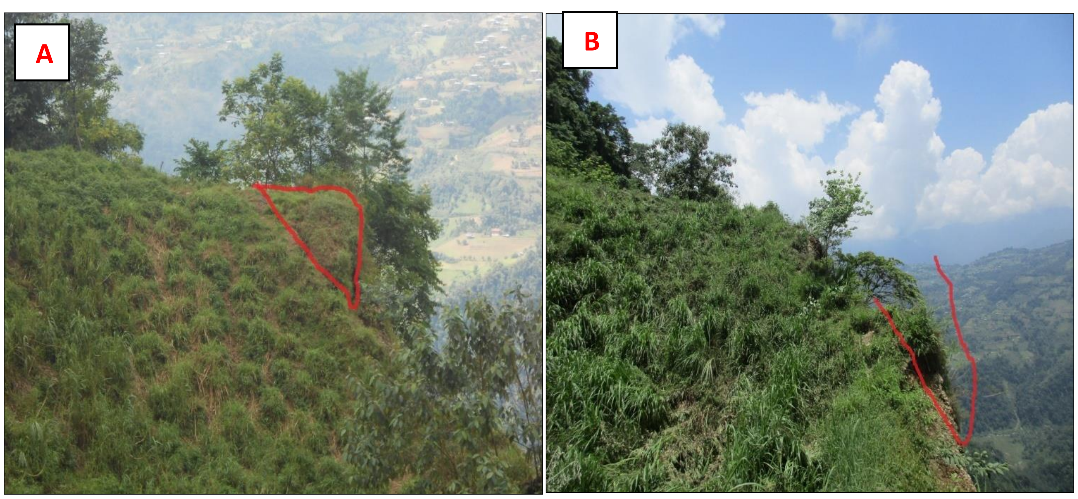

Figure 11. A) Showing the image of tension crack at Arong in August 2015. B) The same site showing the washed away tension crack in May 2016.

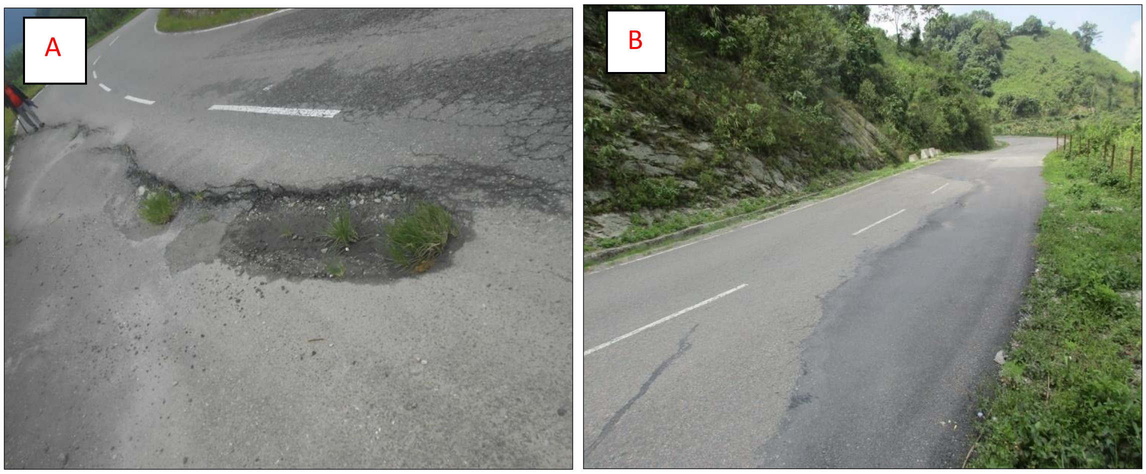

Figure 12. A) The sight of the road at Arong with a clear crack on August 2015. B) The same sight of the road after blacktopping on May 2017.

5.2.2. Moshi Landslide

At Moshi, three tension cracks have been observed and measured during the landslide monitoring. Of the three tension cracks two are located on the road with coordinate N 27.111668°, E 91.5453° and N 27.9031°, E 91.51103° respectively. The dimensions of the crack are 15m by 0.05m and 45m by 0.2m (Table 4).

Figure 13. A) The sight of the road at Moshi with a red line showing the crack on August 2015. B) The same sight of the road after filling up with rock and soil on May 2017 without clear sight of tension crack.

But however, during the next observation, the tension cracks have been covered by the road maintenance agency BRO (Figure 13 A and B). The tension crack with coordinate N 27.11159° and E 91.54421° has the deviation of 0m length and 0.1m width in May 2016 and 2m length and 0.1m width in May 2017 (Table 4).

5.2.3. Phongmey Landslide

At Phongmey, three tension cracks have been observed and measured during the landslide monitoring. Of the three tension cracks one is located on the road with coordinate N 27.3702°, E 91.7419°. The dimension of the crack was noted as 32.40m by 0.31m. However, during the next observation like the above two landslides, the tension cracks have been covered with soil hence making the measurement impossible.

The tension crack with coordinate N 27.3699° and E 91.7423° located below a house has the deviation of 3m and 0.07m in May 2016 and 23m and 0.79m in May 2017 (Table 4). The increased in the height of the fencing below the house shows the evidence of subsidence/movement (Figure 10).

6. CONCLUSIONS

6.1. MOVEMENT OF GPS POINTS

(1) All monitoring points moved between each set of GPS observations (refer Table 3 for movement data and Appendix 9 for figures showing the movement of each point).

(2) Total movement of control points is dominated by seasonal vertical movement compared to seasonal horizontal movement (as can be observed from Table 3)(Anon 2000).

(3) At 10 monitoring points, maximum velocities occurred between April 2016 and October 2016. Minimum velocities at all points occurred between August 2015 and April 2016 (Table 3).

(4) The summary of horizontal and vertical movement (displacement) and movement rate (velocity) is shown in Table 6.

(5) The net average velocity (movement rate) of 0.296 mm per day at Arong landslide falls under very slow to slow category of movement rate as per classification of Varnes (1978).

(6) The net average velocity (movement rate) of 0.150 mm per day at Moshi landslide and Phongmey landslide fall under the extremely slow category of movement rate as per classification of Varnes (1978).

(7) The net average movement rates of the Moshi and Phongmey landslides can be classified as a stable movement (Figure 14) and therefore indicate a normal situation.

(8) The net average movement rate of the Arong landslide can be classified as large seasonal fluctuations (Figure 14) and therefore indicate an alert situation.

(9) However, since the GPS observations are made only on the surface or near-surface of the landslides with only few control points, therefore, monitoring using integrated monitoring systems approach (both contact and remote) that help

determine more representative and accurate movement of these landslides is recommended. This will include but not limited to monitoring using instruments or techniques such as inclinometer, extensometer, piezometer, total stations, and satellite and terrestrial remote sensing.

Table 6. Summary of net horizontal and vertical movement (displacement) and movement rate (velocity)

Description	**Arong**	**Moshi**	**Phongmey**
Net average horizontal movement	0.25 m	0.38 m	0.08 m
Net average vertical movement	1.51 m	0.66 m	0.57 m
Net average velocity (movement rate)	0.296mm/day	0.15mm/day	0.15mm/day

The relationship between the movement rate of landslide and situational or hazard level is shown in Figure 14.

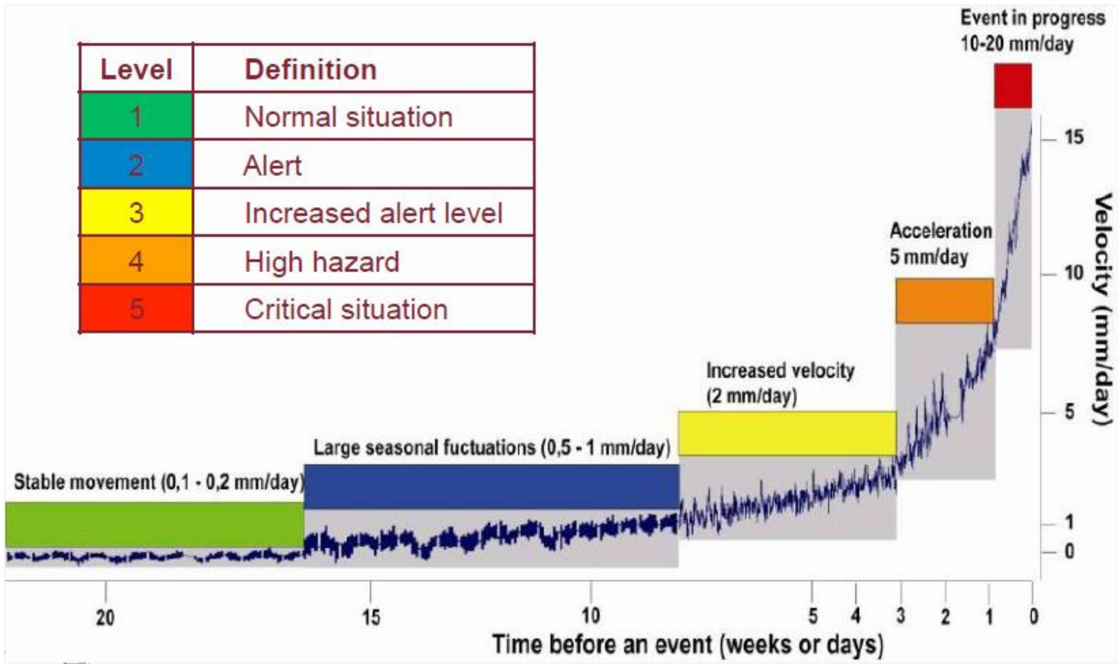

Figure 14. The relationship between landslide movement rate and situational or hazard levels.

6.2. Tension Cracks

Similar to monitoring points for GPS, all the 11 tension cracks showed movement (refer Table 4 for movement data). The change in the length of the tension crack ranges from 0 m for tension crack located in Moshi to 45.1 m for tension crack located in Arong landslide. Similarly, the change in the width of the tension crack ranges from 0.1 m for tension crack in Phongmey, Moshi and Arong to 0.4 m for tension crack in Phongmey (Table 4).

7. ACKNOWLEDGEMENT

The authors are very grateful to Mr Phuntsho Tobgay, Director General; Mr Ugyen Wangda, Chief Geologist of Geological Survey Division; and Mr Tashi Tenzin, Project Manager of DGM for their leadership, support, guidance and feedback provided during fieldwork and report and map preparation. The support and guidance rendered by NAPA-II Project Manager Ms Sonam Lhaden Khandu; current Project Support Officer Mr Netra Sharma and all previous Project Support Officers; Mr Ugyen Dorji; NAPA-II focal person from UNDP; current and past Project Directors from NEC; Board Chair and Members; and all other people who were directly or indirectly involved in this project are well appreciated. Our gratitude also goes to Mr Netra Sharma for improving this report by proof-reading the final draft and providing valuable comments. We also thank Mithun Breeding Centre at Arong, local government, National Center for Hydrology and Meteorology, and all other government agencies, NGOs, private firms and people who have provided help during fieldwork and feedback during the National Workshop held on this project at Phuentsholing from 13-14 November 2017. Lastly, on behalf of DGM, we sincerely extend our gratitude to LDCF-GEF and UNDP for providing funding and technical support, without which, this study would not have been achieved.

8. References

Althuwaynee, O. & Pradhan, B., 2012, Prediction of Slope Failures Using Bivariate Statistical Based Index of Entropy Model. , (Chuser), p. 8–13.

Anon, 1997, 2, Review Of Landslide Hazard And Risk Assessment : , p. 1–56.

Anon, 2000, Seasonal movement of the Slumgullion landslide as determined from Seasonal movement of the Slumgullion landslide as determined from GPS observations , July 1998 - July 1999.

Coe, J.A. & Lidke, D.J., 2003, Seasonal movement of the Slumgullion landslide determined from Global Positioning System surveys and field instrumentation ... Seasonal movement of the Slumgullion landslide determined from Global Positioning System surveys and $ field instrumentation , (August 2017).

Long, S. et al., 2011, Geologic Map of Bhutan, p. 89.

McQuarrie, N. et al., 2013. Documenting basin scale, geometry and provenance through detrital geochemical data: Lessons from the Neoproterozoic to Ordovician Lesser, Greater, and Tethyan Himalayan strata of Bhutan: *Gondwana Research*, 23(4).

Rawat, M.S. et al., 2011. Landslide movement monitoring using GPS technology : A case study of Bakthang landslide , Gangtok , East Sikkim , India. , 3(May), p. 194–200.

Report printed at Kuensel Corporation Ltd., Thimphu: Bhutan